A R C H I V E S O F M E T A L L U R G Y A N D M A T E R I A L S
Volume 60 2015 Issue 1
DOI: 10.1515/amm-2015-0022

G. CIOS*, P. BAŁA*,**, M. STĘPIEŃ*, K. GÓRECKI**

MICROSTRUCTURE OF CAST Ni-Cr-Al-C ALLOY

MIKROSTRUKTURA LANEGO STOPU Z UKŁADU Ni-Cr-Al-C

Nickel based alloys, especially nickel based superalloys have gained the advantage over other alloys in the field of high temperature applications, and thus become irreplaceable at high temperature creep and aggressive corrosion environments, such as jet engines and steam turbines. However, the wear resistance of these alloys is insufficient at high temperatures. This work describes a microstructure of a new cast alloy. The microstructure consists of γ matrix strengthened by γ' fine precipitates (dendrites) improving the high temperature strength and of Chromium Cr_7C_3 primary carbides (in interdendritic eutectics) which are designed to improve wear resistance as well as the high temperature strength.

Keywords: Nickel based alloy, Chromium carbides, cast alloy, wear resistant alloy

Stopy na osnowie niklu, a w szczególności superstopy na osnowie niklu zyskały przewagę w stosunku do innych stopów metali na polu zastosowań w wysokiej temperaturze. Są niezastąpione w warunkach pełzania wysokotemperaturowego, a także agresywnym środowisku korozyjnym silników odrzutowych czy tez turbin parowych. Jednakże odporność na ścieranie tych stopów jest niewystarczalna do zastosowania tych materiałów w wysokiej temperaturze i warunkach ścierania. W niniejszej pracy opisano mikrostrukturę nowego stopu. Składa się ona z osnowy γ umocnionej fazą γ' (dendryty) – zwiększającą wytrzymałość wysokotemperaturową, a także z pierwotnych węglików chromu Cr_7C_3 (w eutektykach międzydentrytycznych) – mających na celu zwiększyć zarówno odporność na ścieranie jak i wytrzymałość wysokotemperaturową.

1. Introduction

Tool steels, among alloys for high temperature applications, are the most popular. However, working at temperatures which are exceeding their tempering temperatures (550÷620°C) causes softening and decreasing of their properties. For example, Titanium alloys at high temperatures are prone to ignition (especially during wear) [3], Nickel based superalloys can withstand temperatures exceeding 1000°C mostly due to γ' (Ni_3Al) strengthening, but the wear resistance is still insufficient [4], and Cobalt based alloys (Stellites) have good high temperature properties and low wear rate at 600÷750°C [5]. Nickel, Cobalt, and Iron based alloys containing high volume fractions of carbides have been already developed, for example, Cr carbides ($Cr_{23}C_6$, Cr_7C_3 and Cr_3C_2), MC type carbides of Hf, Zr, Ta and Nb, or most frequently used with combination of both Cr and MC carbides [6-14]. In the newly developed Nickel based alloy, the triple stage strengthening was applied by chromium carbides, MC carbides, and γ' ($Ni_3(AlTa)$) precipitation hardening known from superalloys [15-17]. Chromium carbides can be classified according to hardness as following: $Cr_{23}C_6$ (976-1650 μHV), Cr_7C_3 (1336-2200 μHV), Cr_3C_2 (1350-2280 μHV), and in reverse order according to fracture toughness [18-20]. Figure 1a shows the ternary Ni-Cr-C solidus projection. It is shown that the Ni as solid solution + Cr_3C_2 (blue line) is solidifying in a small field in the Ni-rich corner in the vicinity of Ni + Cr_2C_3+ graphite field. On the other hand the Ni + Cr_7C_3(red line) field is very wide in the Ni-rich corner of the diagram. After solidification, solubility of carbon in nickel solid solution matrix is decreasing, therefore fields of carbon rich phases are shifted towards lower Carbon content at 1200°C and 1000°C as shown in Figure 2.

The aim of the present study is to characterize the microstructure of the as-cast state quaternary Ni-Cr-Al-C alloy and to assess its ability to γ' precipitation hardening.

2. Experimental procedure

The cross-sections of the investigated material ingot was polished and etched using modified Marbles reagent. The microstructure of the material was examined by Nikon LV150N light microscope and FEI VERSA 3D scanning electron microscope. The X-Ray diffraction (XRD) was performed by Panalytical Empyrean diffractometer using Cu$K\alpha_1$ radiation (λ =1.5405 Å). Hardness tests were performed by TUKON 2500 hardness tester using the Vickers hardness test.

* AGH UNIVERSITY OF SCIENCE AND TECHNOLOGY, ACADEMIC CENTRE FOR MATERIALS AND NANOTECHNOLOGY, AL. A. MICKIEWICZA 30, 30-059 KRAKÓW, POLAND
** AGH UNIVERSITY OF SCIENCE AND TECHNOLOGY, FACULTY OF METALS ENGINEERING AND INDUSTRIAL COMPUTER SCIENCE, AL. A. MICKIEWICZA 30, 30-059 KRAKÓW, POLAND

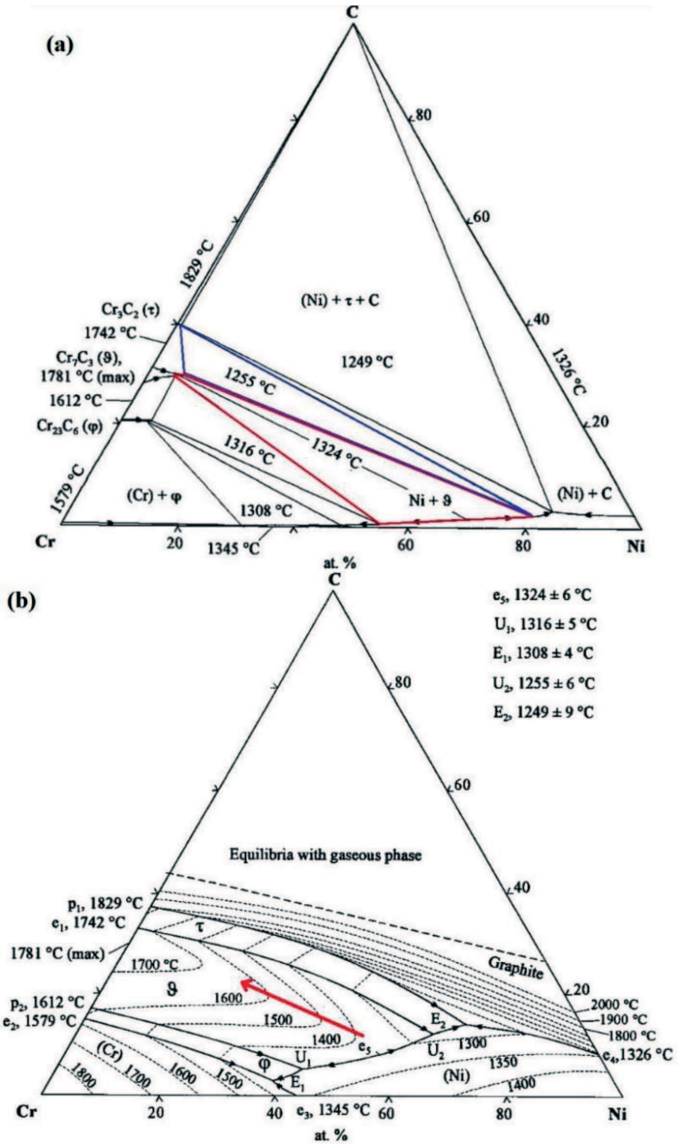

Fig. 1. Solidus (a) and liquidus (b) projection of Ni-Cr-C ternary diagram [14]

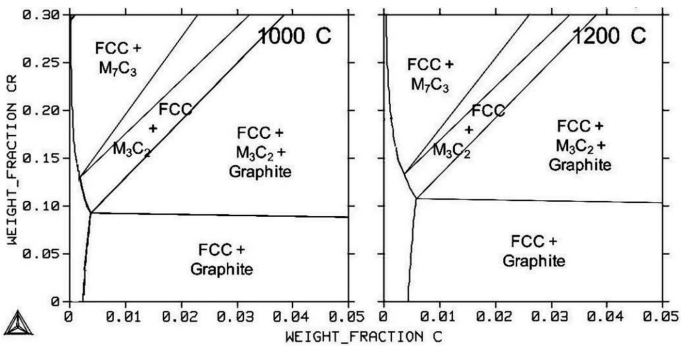

Fig. 2. Pseudo-binary isothermal cross-sections of Ni-Cr-C ternary diagram

3. Material

Investigated alloy was melted in vacuum furnace Balzers VSG-02 and then cast into metal chills. The chemical composition of the alloy is included in Table 1.

TABLE 1
Chemical composition of investigated alloy (mass %)

C	Cr	Al	Ni
0.85	20	3	balance

4. Results and discussion

The microstructure of the investigated alloy is presented in Figure 3 a) and b). It can be observed that the alloy consists of large grains with dendritic structure. Primary dendrites with secondary branches can are also visible. Chromium carbides are situated in primary eutectic in interdendritic zones (Figure 4) as well as in dendrites (Figure 5). The γ' (Ni_3Al) phase is present after solidification in form of two morphologies: coarsed primary precipitates between carbides in interdendritic zones and fine secondary precipitated during cooling of the ingot (Figure 6). The X-Ray diffraction analysis revealed that chromium carbides are orthorhombic Cr_7C_3 and confirmed that the γ' phase is present (Figure 7). It should be emphasized that the high purity alloy was successfully synthesized in the study. This alloy does not contain neither sulphides nor zones of the γ/γ' eutectic which are characteristic for Ni-based superalloys in as-cast condition. The average hardness of the investigated alloy is 286±8 HV10.

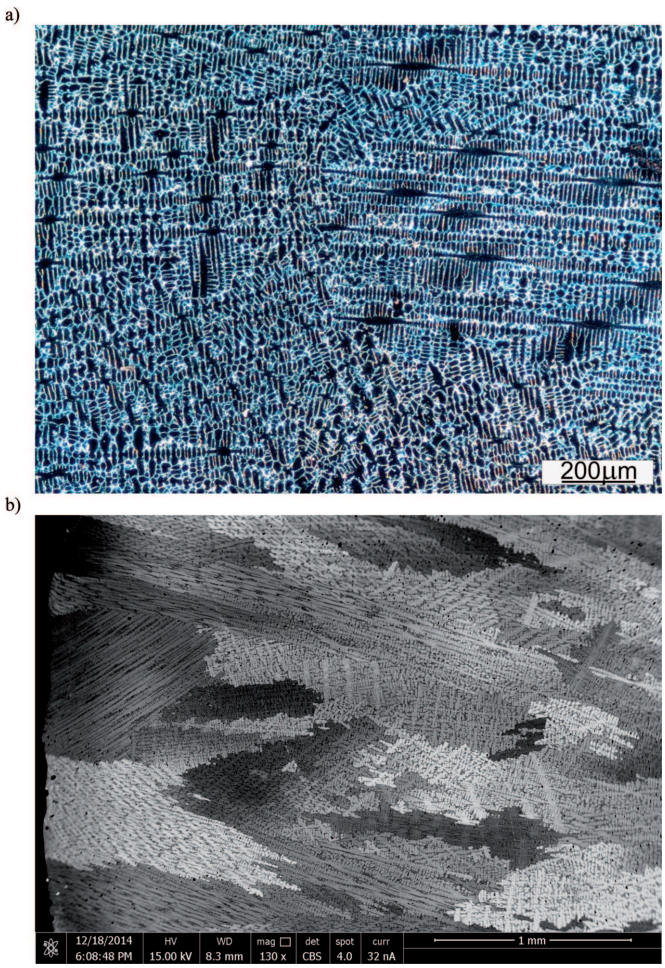

Fig. 3. Microstructure of investigated alloy ingot a) light microscope dark field image b) SEM-BSE image

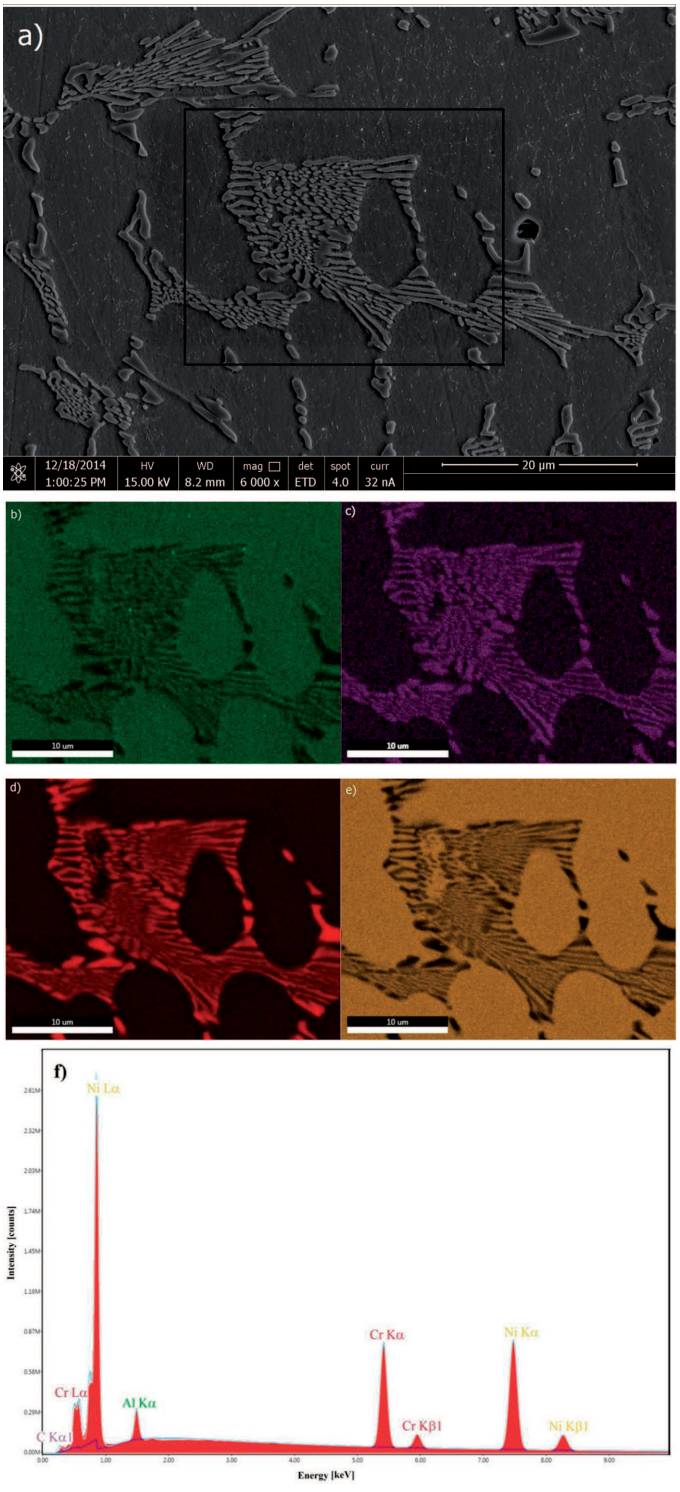

Fig. 4. Microstructure of investigated alloy a) SE image with EDS analysis area, b) c) d) e) show particular elements Aluminum, Carbon, Chromium and Nickel maps, respectively, f) EDS spectrum of the area

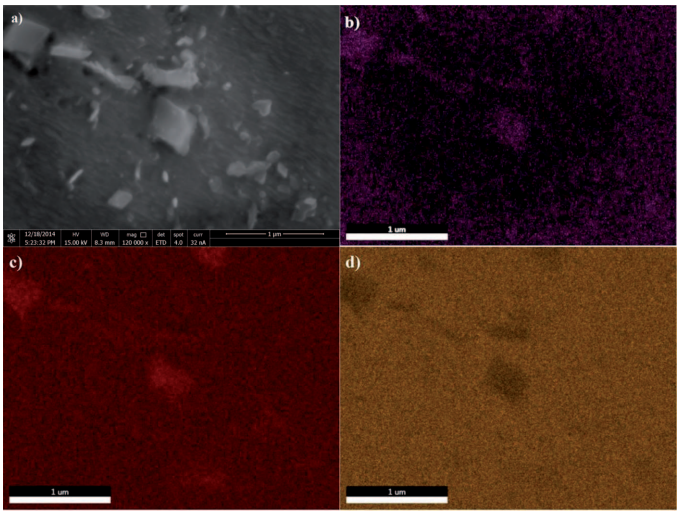

Fig. 5. Microstructure of secondary carbides in dendrites in investigated alloy a) SE image, b), c), and d) EDS maps of carbon, chromium, and nickel, respectively

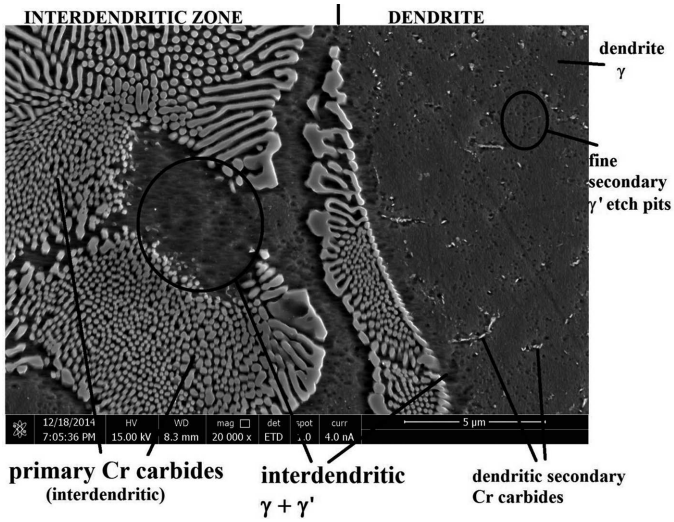

Fig. 6. SEM-SE image showing microstructure of the investigated alloy

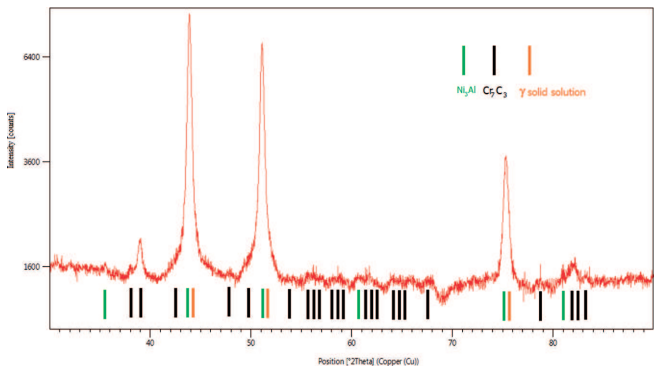

Fig. 7. XRD analysis of the investigated alloy

5. Conclusions

1. Microstructure of the investigated alloy consists of large grains with dendritic structure.
2. Dendrites mainly consists of γ solid solution with γ' and Cr_7C_3 secondary precipitates.
3. Interdendritic zones contain eutectic chromium carbides (Cr_7C_3) and coarsed γ' precipitates encircled with γ phase channels.
4. Neither graphite nor γ/γ' eutectics are present in the alloy, what indicates proper balance between carbon and chromium content, as well as an adequate content of aluminum.
5. Results obtained during the study did not show any of solidification cracks and nonmetallic inclusions present in the alloy.
6. The investigated alloy in the as-cast state is precipitation hardened by γ'.

REFERENCES

[1] P. Bała, J. Pacyna, Arch. Metall. Mater. **53**, 795 (2008).
[2] P. Bała, J. Pacyna, J. Krawczyk, Kov. Mater. Mater. **49**, 125 (2011).
[3] M. Guang-Bao, H. Xu, C. Jing-Xia, C. Chun-Xiao, H. Xiu-song, Trans. Nonferrous Met. Soc. China Nonferrous Met. Soc. China **23**, 2270-2275 (2012).
[4] R.C. Reed, The Superalloys Fundamentals and Applications, Cambridge 2006.
[5] S.-T. Chen, W.Y. Tang, Y.F. Kuo, S.Y. Chen, C.H. Tsau, T.T. Shun, J.W. Yeh, Mater. Sci. Eng. A **527**, 5818 (2010).
[6] L. Aranda, P. Berthod, Y. Hamini, Comput. Coupling Phase Diagrams Thermochem. **31**, 361 (2007).
[7] P. Berthod, Mater. Corros. **5**, 567 (2013).
[8] P. Berthod, Y. Hamini, L. Aranda, Comput. Coupling Phase Diagrams Thermochem. **31**, 351 (2007).
[9] P. Berthod, E. Conrath, Adv. Alloy. Compd. **1**, 3 (2014).
[10] P. Berthod, L. Aranda, Y. Hamini, Mater. Sci. **47**, 319 (2011).
[11] P. Berthod, J. Alloys Compd. **481**, 746 (2009).
[12] P. Berthod, P. Lemoine, J. Ravaux, J. Alloys Compd. **467**, 227 (2009).
[13] P. Berthod, L. Aranda, C. Vébert, S. Michon, Comput. Coupling Phase Diagrams Thermochem. **28**, 159 (2004).
[14] T.Y. Velikanova, A.A. Bondar, A.V. Grytsiv, J. Phase Equilibria **20**, 125 (1999).
[15] P. Bała, Arch. Metall. Mater. **57**, 937 (2012).
[16] P. Bała, Arch. Metall. Mater. **55**, 1053 (2010).
[17] P. Bała, Arch. Metall. Mater. **59**, 977 (2014).
[18] W.S. da Silva, R.M. Souza, J.D.B. Mello, H. Goldenstein, Wear **271**, 1819 (2011).
[19] R. Chattopadhyay, Surface Wear: Analysis, Treatment, and Prevention. Materials Park OH, 2001.
[20] A. Zikin, I. Hussainova, C. Katsich, E. Badisch, C. Tomastik, Surf. Coatings Technol. **206**, 4270 (2012).

Received: 20 March 2014.